01 Jan 2006

Intelligent Tool for Determining the True Harmonic Current Contribution of a Customer in a Power Distribution Network

Joy Mazumdar

Frank C. Lambert

Ganesh K. Venayagamoorthy
Missouri University of Science and Technology

Marty L. Page

et. al. For a complete list of authors, see https://scholarsmine.mst.edu/ele_comeng_facwork/1692

Recommended Citation

J. Mazumdar et al., "Intelligent Tool for Determining the True Harmonic Current Contribution of a Customer in a Power Distribution Network," *Conference Record of the 41st IAS Annual Meeting of the Industry Applications Conference, 2006*, Institute of Electrical and Electronics Engineers (IEEE), Jan 2006. The definitive version is available at https://doi.org/10.1109/IAS.2006.256597

Intelligent Tool for Determining the True Harmonic Current Contribution of a Customer in a Power Distribution Network

J.Mazumdar, R.Harley, F.Lambert
School of Electrical Engineering
Georgia Institute of Technology
Atlanta, GA 30332-0250 USA
joymazum@ece.gatech.edu

G.K.Venayagamoorthy
RTPIS Laboratory
University of Missouri-Rolla
Rolla, MO 65409-0249 USA
gkumar@ieee.org

M.L.Page
Distribution Reliability and Management
Georgia Power Company
Atlanta, GA 30308-3374 USA
malpage@southernco.com

***Abstract*—Customer loads connected to electricity supply systems may be broadly categorized as either linear or nonlinear. Nonlinear loads inject harmonics into the power network. Harmonics in a power system are classified as either load harmonics or as supply harmonics depending on their origin. The source impedance also impacts the harmonic current flowing in the network. Hence any change in the source impedance is reflected in the harmonic spectrum of the current. This paper proposes a novel method based on Artificial Neural Networks to isolate and evaluate the impact of the source impedance change without disrupting the operation of any load, by using actual field data. The test site chosen for this study has a significant amount of triplen harmonics in the current. By processing the acquired data with the proposed algorithm, the actual load harmonic contribution of the customer is predicted. Experimental results confirm that attempting to predict the total harmonic distortion (THD) of a customer by simply measuring the customer's current may not be accurate. The main advantage of this method is that only waveforms of voltages and currents at the point of common coupling have to be measured. This method is applicable for both single and three phase loads.**

Keywords-power system harmonics; harmonic analysis; neural networks; power quality; total harmonic distortion

I. INTRODUCTION

The dependence of modern life upon the continuous supply of electrical energy makes system reliability and power quality topics of utmost importance in the area of power system research. Modern day industrial applications extensively use power electronic devices. They have proven to be extremely useful but, unfortunately, the current waveforms that these devices produce are not sinusoidal [1]. The presence of current and voltage harmonics in power distribution systems increases losses in lines, decreases the power factor, and can even cause resonance with capacitors connected in parallel to the system. Present equipment setups and devices used in commercial and industrial facilities, such as digital computers, automated equipments, etc are extremely sensitive to harmonics [2]. As a result, power quality in recent years has become an important issue and is receiving increasing attention by utility, customer, and consulting engineers.

This project was supported by the National Electric Energy Testing Research and Applications Center (NEETRAC), Georgia, USA.

Harmonics-related problems on electric utility distribution systems are usually created by primary metered customers. The significant harmonics are mostly 5^{th}, 7^{th}, 11^{th} and 13^{th} with the 5^{th} harmonic the largest in most cases. Classic utility-side symptoms of harmonics problems are distorted voltage waveforms, blown shunt capacitor fuses, and transformer overheating. Capacitor losses are sensitive to harmonic voltages. Transformer losses are sensitive to harmonic currents.

In 1981, the IEEE 519 harmonic standard was issued as a guideline for harmonic related issues. The standard was revised in 1992 [3], [4]. IEEE 519 attempts to establish reasonable harmonic goals for electrical systems that contain nonlinear loads. The objective is to propose steady-state harmonic limits that are considered reasonable by both electric utilities and their customers. IEEE 519 standard is a recommended practice, not an enforced law, although it is being increasingly applied as such [5].

A typical one line diagram of a power distribution network is shown in Fig. 1. If the nonlinear load is supplied from a sinusoidal voltage source, its injected harmonic current $i_{abc}(t)$ is referred to as *contributions from the load,* or load harmonics. Harmonic currents cause harmonic volt drops in the supply network. Any other loads, even linear loads, connected to the point of common coupling (PCC) have harmonic currents injected into them by the distorted PCC voltage. Such currents are referred to as *contributions from the power system*, or supply harmonics.

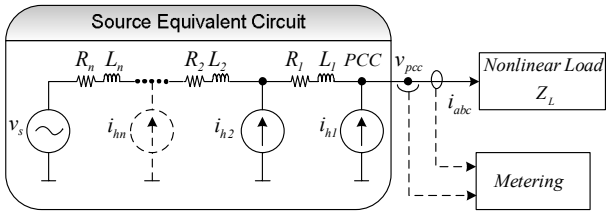

Figure 1. Typical one line diagram of a power distribution network

If several customers are connected to a PCC, it is not possible by traditional methods [6], [7] to accurately determine the amount of harmonic current injected by each customer, in order to tell which customer(s) is injecting the excessively high

harmonic currents, or whether the source is responsible for the harmonics by the virtue of a distorted PCC voltage.

To mitigate the effects of harmonic currents, harmonic filtering has been a standard solution adopted by industry [8]. Harmonic filters are mainly classified as *passive filters* and *active filters*. Passive L-C tuned filters are used to absorb the harmonic currents generated by nonlinear loads. Active filters, on the other hand, are based on PWM current or PWM voltage source inverters, which are controlled to stop the flow of harmonic current from the nonlinear load to the utility system [9], [10]. At this point, the issue of harmonic resonance warrants special attention. Installed L-C tuned filters may resonate with the system impedance. Resonance occurs when the harmonic currents injected by nonlinear loads interact with system impedances to produce high harmonic voltages. Resonance can cause nuisance tripping of sensitive electronic loads and high harmonic currents in feeder capacitor banks. In severe cases, capacitors produce audible noise and sometimes even bulge. Under these circumstances, utilities sometimes change the source impedance by switching capacitor banks. Changing the source impedance components, such as transformer impedance or system impedance, on a distribution system, detunes the system. This can have a significant impact on the harmonic content of the current flowing in the network [11]. In general, higher source impedance yields higher voltage harmonics.

This paper addresses the issues related to the change of source impedance by a utility and how it impacts the power system network harmonics based on field data gathered at a substation in Georgia, USA. The test site chosen is primarily a residential feeder. Furthermore, this paper demonstrates the application of neural networks to predict the true harmonic current distortion of the customer under a specific resonance condition in the distribution system and validates the prediction when the utility changes the source impedance to remove the resonance condition.

II. Analysis of Acquired Data

The distribution system configuration at the measurement site is a 3 phase 4 wire wye connection. Waveforms of phase A line-neutral voltage and the three line currents are acquired as 6 cycle snapshots, every 20 seconds, for a period $2^1/_2$ hours. Each snapshot measurement is designated as an event. Hence 462 events are recorded. The sampling frequency for data acquisition is set at 256 samples per cycle. All data acquisition is done at the substation as shown in Fig. 2. The measurement instrument acquires binary data files. The software import converts the data to text readable format.

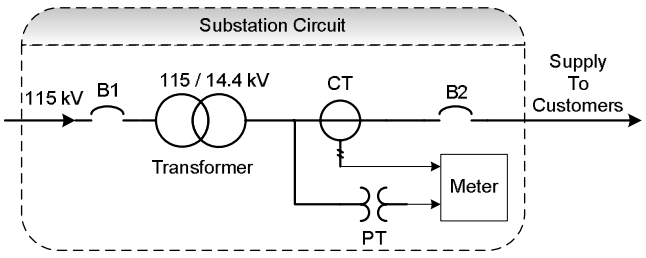

Figure 2. Substation circuit and data acquisition schematic

A 20 ampere full scale clamp on the CT is used, measuring only about 0.25 amps in the relay circuit of the feeder breaker. The current therefore already reflects the CT ratios and represents the current in primary line values. The voltage is a 120 volt measurement of a 25 kV line-line (14.4 kV line to neutral) service. Hence, a PT ratio of 14400/120 is applied.

Figure 3 shows the variation of the current THD for the three line currents over the entire period of measurement.

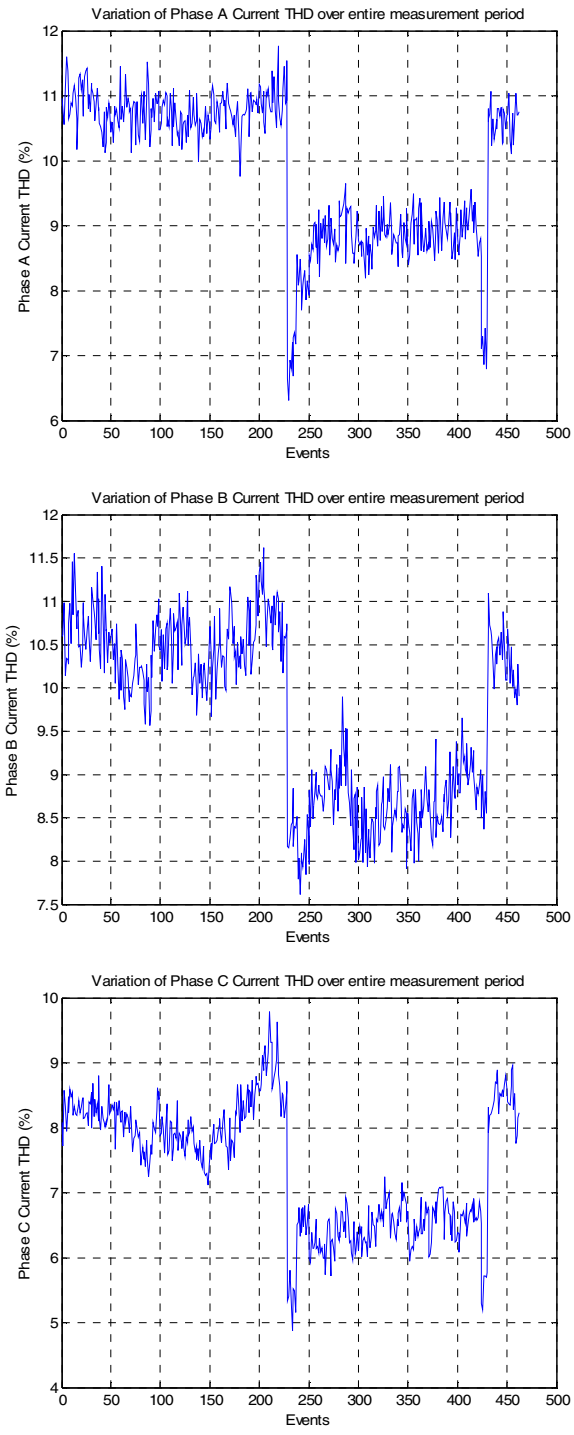

Figure 3. Variation of current THD for the three line currents

The THD values for the three line currents undergo a step change during event 238. This is the point when the utility switched some capacitor banks in the substation to effect a change in the source impedance. The phase A and phase B currents had THD's in the range of 10.5~11% before the source impedance changed and after the change, the THD's dropped to values between 8.5~9%. The phase C current THD before and after the impedance change was 8% and 6.5% respectively.

Figure 4 shows the variation of the voltage THD for phase A over the entire period of measurement.

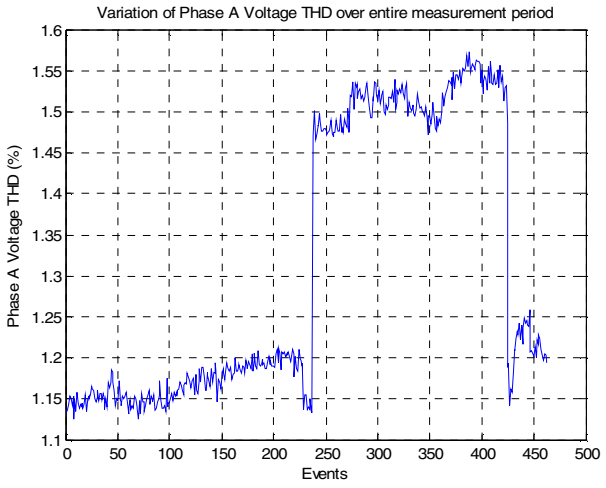

Figure 4. Variation of phase A voltage THD

The voltage THD is well within the limits specified by IEEE 519 even after the small step increase when the impedance change is made.

Figure 5 shows six cycles of the actual phase A voltage and current waveform acquired **before** the impedance change.

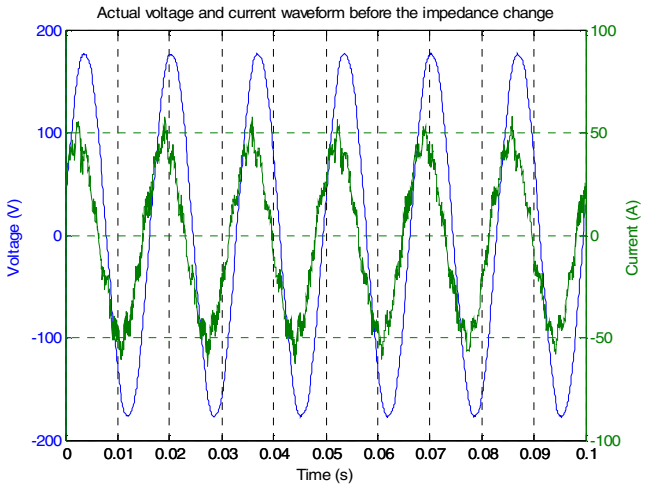

Figure 5. Six cycles of acquired voltage and current waveform before the impedance change

The voltage waveform in Fig. 5 appears clean, while the current waveform is extremely noisy. Noisy current waveforms with high harmonic content result in telephone interference and the same was reported from this site. The Fourier spectrum of the current waveform in Fig. 5 is shown in Fig. 6 with a dominant 9^{th} harmonic.

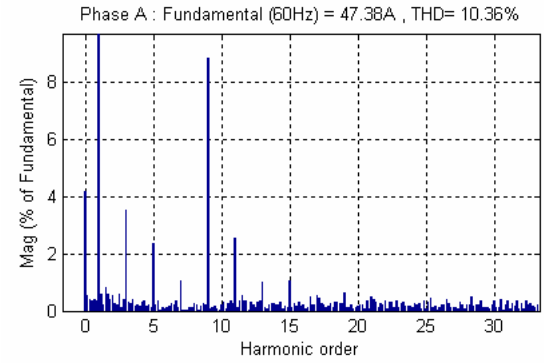

Figure 6. FFT plot of phase A current before source impedance change

Figure 7 shows six cycles of the phase A voltage and current waveforms **after** the impedance change. The current waveform in Fig. 7 is still noisy after the impedance change; however the harmonic spectrum (Fig. 8) of the current has changed.

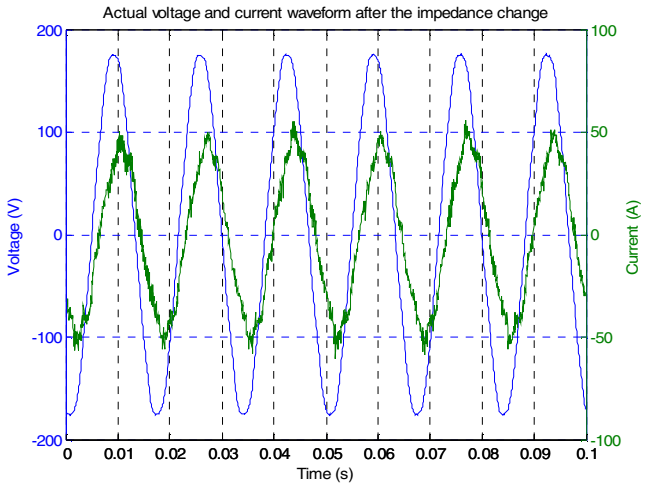

Figure 7. Six cycles of acquired voltage and current waveform after the impedance change

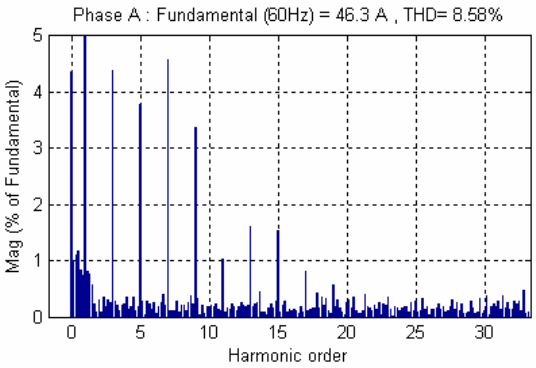

Figure 8. FFT plot of phase A current after source impedance change

Some observations can be made from the above plots. There is a DC offset present in the current waveform and the current is rich in high frequency components. In particular the 9^{th} harmonic dominates and causes telephone interference on a street served by this feeder, which is the reason why this particular circuit is chosen for analysis. The above results indicate a possible network resonance. The switching in the substation changes the source impedance and causes a reduction in the 9^{th} harmonic as shown in Fig. 8. A high 9^{th} harmonic is often the result of a single fuse blown on a three phase capacitor bank, but in this case no fuses blew. However, there are some subdivision loads with underground service and therefore, cable capacitance is present. Whatever may be the cause [12], the customer current has triplen harmonics and the customer could be held responsible to take corrective actions to rectify the same [13], [14], unless it could be proven that these triplen harmonics cannot be attributed to the customer.

III. ESTIMATION OF HARMONIC CURRENT

Artificial Neural Networks (ANNs) have provided an alternative modeling approach for power system applications. The multilayer perceptron network (MLPN) is one of the most popular topologies in use today [15]. This paper uses a method based on MLPN to predict the true harmonic current distortion that can be attributed to a customer, without disrupting the operation of any customer. The method was originally proposed in [16]. A single line diagram, consisting of the utility equivalent circuit, the customer and the neural network based Load Model Identifier (LMI) is shown in Fig. 9. The utility equivalent circuit comprises of a three-phase supply network having a sinusoidal voltage source v_s, network impedance L_s, R_s and several other loads, which can be linear or nonlinear. The LMI consists of two individual neural network blocks, the **identification** neural network (ANN1) and the **estimation** neural network (ANN2). The voltage v_{abc} and current i_{abc} at the service entrance of the customer are the parameters of interest and are processed by the LMI.

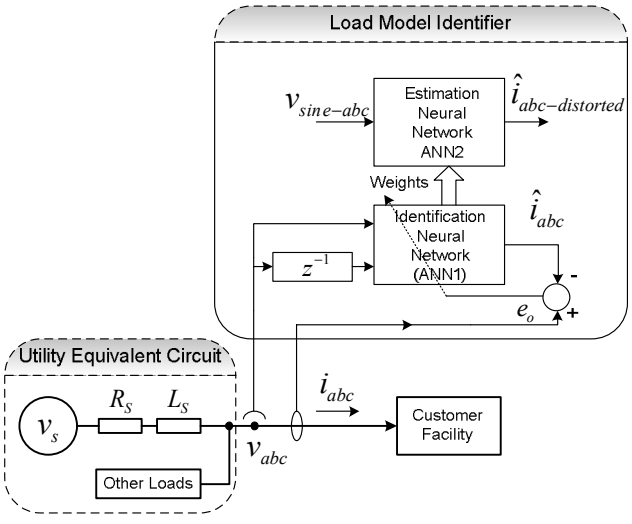

Figure 9. Harmonic current prediction scheme

A. Brief description of the scheme

The customer's load currents i_a, i_b, and i_c, (denoted by i_{abc}), are composed of load harmonics as well as supply harmonics. However, the utility sees the line current i_{abc} as the harmonic distortion injected into the network by the load. ANN1 is trained to **identify** the nonlinear characteristics of the load (in the case of a single phase load), and for each phase individually for a three-phase load. At any moment in time after the ANN1 training has been completed, its weights are transferred to ANN2. ANN2 is then supplied offline with a three-phase mathematically generated sine-wave $v_{sine-abc}$ to estimate its three output currents $\hat{i}_{abc-distorted}$. Any distortion present in the current waveforms $\hat{i}_{abc-distorted}$ can now truly be attributed to the nonlinearity of the load admittance. This procedure is known as load modeling. ANN2 is a replica of the trained ANN1 structurally. The function of ANN2 could have been carried out by ANN1, but that would disrupt the continual online training of ANN1 during the brief moments when $\hat{i}_{abc-distorted}$ has to be estimated. The algorithms of ANN1 and ANN2 are executed in software.

B. Operation of the Identification Neural Network (ANN1)

The proposed method measures the instantaneous values of the three voltages v_{abc} at the PCC, as well as the three line currents i_{abc} at the k^{th} moment in time. The voltages v_{abc} could be line-to-line or line-to-neutral measurements. The ANN1 is designed to predict one step ahead the line current $\hat{i}_{abc}$ as a function of the present and delayed voltage vector values $v_{abc}(k)$, $v_{abc}(k-1)$ and $v_{abc}(k-2)$. When the $(k+1)^{th}$ moment arrives (at the next sampling instant), the actual measured instantaneous values of i_{abc} are compared with the previously predicted values of $\hat{i}_{abc}$, and the error e_o is used to train the ANN1 weights. This ensures continual online training of ANN1.

Initially the weights have random values, but after several sampling steps, the training soon converges and the value of the error e_o in Fig. 9 diminishes to an acceptably small value, as expressed by the value of mean squared error in (8). Proof of this is illustrated by the fact that the individual phase waveforms for i_{abc} and $\hat{i}_{abc}$ should practically lie on top of each other respectively. At this point the ANN1 therefore represents the admittance of the nonlinear load. This process is called *identifying* the load admittance. Since continual online training is used, it will correctly represent the load admittance from moment to moment. At any moment in time after the ANN1 training has converged, its weights are transferred to ANN2. The training cycle of ANN1 continues to follow load changes and in this way ANN2 always has updated weights available when needed.

C. Operation of the Estimation Neural Network(ANN2)

The estimation neural network ANN2 is supplied with a mathematically generated sine-wave to estimate its output. The

output of ANN2 called $\hat{i}_{abc-distorted}$ therefore represents the current that the nonlinear load would have drawn had it been supplied by a sinusoidal voltage source. Any distortion present in $\hat{i}_{abc-distorted}$ can now truly be attributed to the nonlinearity of the load admittance.

Once a number of $\hat{i}_{abc-distorted}$ cycles have been calculated by ANN2, they are stored (and subsequently used for harmonic analysis to find the true load-injected current total harmonic distortion THD_i). New weights are then uploaded from ANN1 to ANN2, and a series of new $\hat{i}_{abc-distorted}$ cycles and a new THD_i are calculated. This THD_i value may be recorded or displayed at frequent pre-determined intervals, or an average value calculated over a period of time.

Due to the nature of the sigmoidal transfer function, the outputs of the neurons in the hidden layer are limited to values between 0 and 1. The inputs to the neural networks are therefore first scaled to fall within the limits of ± 1. The scaling of the acquired data is done using software and hence that removes any limitations whatsoever on the data acquisition system and the transducers.

D. ANN Governing Equations

The structure of a MLPN is shown in Fig. 10. This network consists of a set of input neurons, output neurons and one or more hidden layers of intermediate neurons. Data flows into the network through the input layer, passes through the hidden layer and finally flows out of the network through the output layer. The network thus has a simple interpretation as a form of input-output model, with network weights as free parameters.

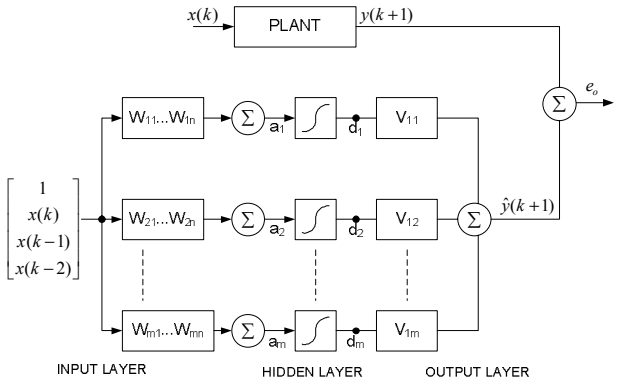

Figure 10. Structure of a MLPN

The process of passing the inputs in Fig. 10 through the neural network structure to its output is known as forward propagation. Every input in the input column vector $\underline{x}$ is fed via the corresponding weight in the input weight matrix W to every node in the hidden layer to determine the activation vector $\underline{a}$. Each of the hidden neuron activations in $\underline{a}$ is then passed through a sigmoidal function to determine the hidden-layer decision vector $\underline{d}$.

$$\underline{a} = W\underline{x} \tag{1}$$

$$d_i = \frac{1}{1+e^{(-a_i)}},\ i \in \{1,2,....,m\} \tag{2}$$

where the input column vector $\underline{x} \in R^n$, the hidden layer activation column vector $\underline{a} \in R^m$, the input weight matrix $W \in R^{m \times n}$, n is the number of inputs to the ANN including the bias and m is the number of neurons in the hidden-layer. The elements of the decision vector $\underline{d}$ are then fed to the corresponding weight in the output weight matrix V.

The ANN output is computed as

$$\hat{y} = (V\underline{d})^T \tag{3}$$

For a single output system, the output weight matrix $V \in R^{1 \times m}$ and $\hat{y}$ is a scalar.

The output error is calculated as

$$e_o = y - \hat{y} \tag{4}$$

The process of passing the output error to the input in order to estimate the individual contribution of each weight in the network to the final output error is known as error backpropagation [17]. The weights are then modified so as to reduce the output error. The change in input weights ΔW and output weights ΔV at step k are calculated as

$$\Delta W(k) = \gamma_m \Delta W(k-1) + \gamma_g \underline{e}_a \underline{x}^T$$

$$\Delta V(k) = \gamma_m \Delta V + \gamma_g \underline{e}_y \underline{d}^T \tag{5}$$

where $\gamma_m, \gamma_g \in [0,1]$ are the momentum and learning gain constants respectively. The last step in the training process is the actual updating of the weights at step k

$$W(k) = W(k-1) + \Delta W(k)$$

$$V(k) = V(k-1) + \Delta V(k) \tag{6}$$

E. Selection of optimal number of neurons for hidden layer

To model the harmonic characteristics of a nonlinear load, the ANN architecture needs to address the issues regarding,

(1) the number of layers,

(2) number of neurons in each layer, and

(3) the hidden layer activation function.

For any nonlinear function identification type problem, at least one hidden layer is required. Additionally, a nonlinear, continuously differentiable hidden layer activation function, such as the sigmoidal function, allows the network to perform nonlinear modeling. Depending on the application, the number of ANN inputs and the number of outputs are fixed. The only structural variable then remaining is the number of neurons m in the hidden layer. The ANN execution time and the training convergence is directly dependent on the value of m. Two

performance criteria for the measure of ANN training convergence are typically used; they are the absolute value of the tracking error T_e defined as

$$T_e = |(y - \hat{y})| \tag{7}$$

and the Mean Squared Error (MSE) defined as

$$MSE = \frac{1}{r}\sum_{1}^{r}|(y - \hat{y})|^2 \tag{8}$$

where r is the number of training epochs. The tracking error T_e varies at a high rate as training progresses. For this reason it is more convenient to consider the MSE which is a smooth curve due to the averaging process. In neural network training it is not possible to get the MSE to be exactly zero, so the objective is to get it down below some minimum value, typically ($MSE_{min} < 10^{-2}$). This can be achieved by providing information to the neural network about the history of the system dynamics, typically in the form of delayed inputs and outputs.

The number of neurons in the hidden layer affects the rate and the final value of the MSE convergence, and is typically chosen on a heuristic basis after several iterations. For the specific problem presented in this paper, based on experimental data and experience, the following formula provides a starting point for choosing the number of neurons in the hidden layer.

$$H_n \approx \frac{K * n}{C \cdot S \cdot MSE_{min}} \tag{9}$$

where H_n is the number of neurons in the hidden layer, C is the number of cycles of training data, MSE_{min} is the acceptable MSE in training, S is the number of samples per cycle of the acquired data, n is the number of inputs and K is a constant depending on the number of inputs used and the sampling frequency of data . The above formula has been adapted from work of Baum and Haussler [18].

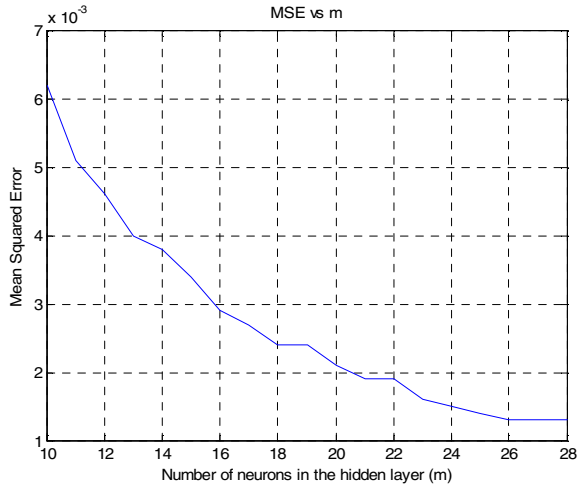

Figure 11. Variation of MSE over different values of the number of neurons in the hidden layer for ANN1

The data acquisition meter used at the site is an AVO Megger PA-9Plus meter with data sampling set at 256 samples/ cycle. Starting with random initial values for the ANN weights, and to achieve a MSE_{min} of 0.2% with data from 1 event (i.e. 6 cycles), the value of K comes out to be 24. Substituting these values in (9), the value of H_n is 23. Figure 11 shows the value of MSE for ANN1 obtained experimentally for different values of neurons in the hidden layer. For the work presented in this paper, the number of neurons used in the hidden layer is 20.

IV. Experimental Results

A. Before source impedance change

The method of using online trained ANNs to identify the load admittance and utilizing the trained neural network to estimate the true harmonic current injection of a customer, is demonstrated with the help of field data.

The text readable field data from the AVO Megger PA-9Plus meter is imported to MATLAB and is passed on to the neural network code. The powergui block of Simulink is used to calculate the voltage and current THD's. These THD's are then compared with values computed directly by the field instrument, in order to verify that both the values are the same.

The phase A voltage and current data in Fig. 4 is used as the pilot data since that has the highest 9^{th} order harmonic and also has the highest harmonic current distortion. This data is passed through a second order lowpass filter (implemented in Simulink) with cutoff frequency $f_c = 2\,kHz$ in order to eliminate the high frequency components. The conditioned data is used to train the neural network ANN1 until the training error converges to near zero, and the output of ANN1 $\hat{i}_a$ correctly tracks the actual phase A current i_a of the customer. Figure 12 indicates how well ANN1 has converged since its output $\hat{i}_a$ coincides with the actual i_a waveform.

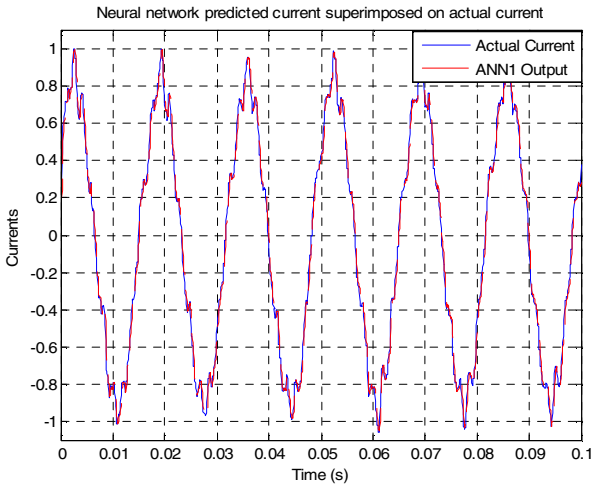

Figure 12. Demonstration of ANN1 training: waveforms of i_a and $\hat{i}_a$ coincide

The convergence of the training can also be verified by considering the Mean Squared Error MSE in Fig. 13 which has a value less than 10^{-2} and almost constant after 400 epochs.

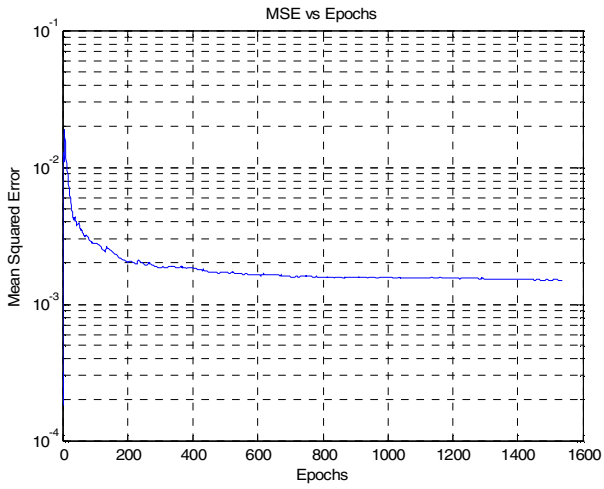

Figure 13. Measure of ANN1 training convergence: MSE in current training

Once the training error is below a pre-defined level $MSE_{\min}$ $(<10^{-2})$, it can be concluded that ANN1 has learned the admittance of the customer load to an acceptable level of accuracy. The weights of ANN1 are now transferred to ANN2. While the ANN1 training continues, the computations of ANN2 are done offline. ANN2 is now supplied with a mathematically generated sine-wave voltage with zero distortion as its input. This is equivalent to the situation wherein the customer is getting a clean sine-wave voltage at its service entrance and the resonance point in the line along with other disturbances and supply harmonics are being avoided. Any load serviced by a utility is designed and optimized to operate at 60 Hz, however once it is connected to the power system network, it rarely receives a clean 60 Hz supply. The output of ANN2 is $\hat{i}_{a-distorted}$ and is shown in Fig. 14.

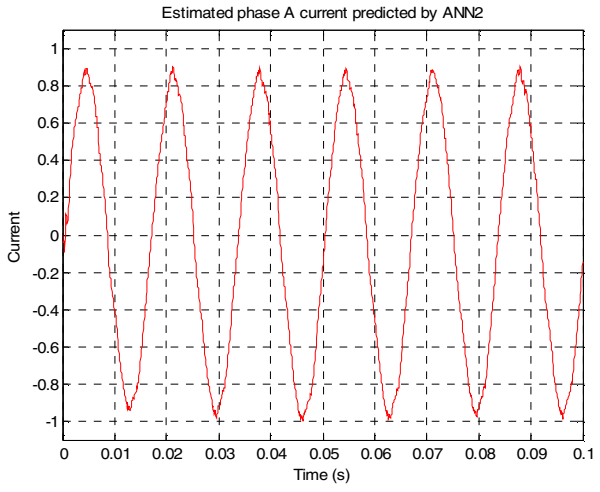

Figure 14. Estimated phase A current when supplied with clean sine-wave

In other words, the $\hat{i}_{a-distorted}$ waveform gives the same information that could have been obtained by quickly removing the customer from the line (if this were possible) and connecting a pure sinusoidal voltage source to the service entrance of the customer, except that it is not necessary to actually do this interruption. The frequency spectrum of the $\hat{i}_{a-distorted}$ waveform is shown in Fig. 15.

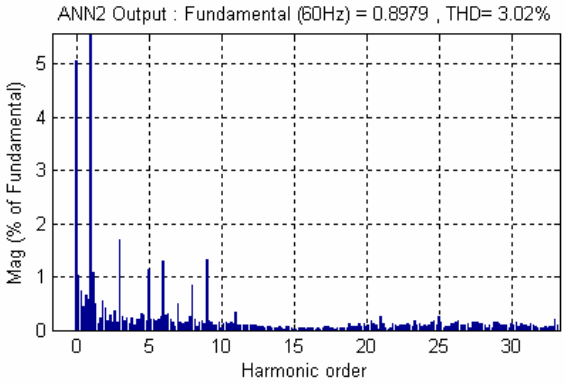

Figure 15. FFT spectrum of the ANN2 predicted current waveform

The true current distortion of the customer turns out to be **3.02%** in Fig. 15 instead of the **10.36%** of Fig. 6. However a more significant finding from the FFT spectrum is the reduction of the 9^{th} harmonic from **8.5%** to about **1.5%** of the fundamental.

B. After source impedance change

The source impedance switching by the utility detunes the resonance point in the feeder and that results in the reduction of the 9^{th} harmonic from **8.5%** to about **3.5%** of the fundamental, as shown in Fig. 8. This result does show that for the particular operating point of the feeder, a resonance condition has a detrimental effect on the power distribution network and triggers the 9^{th} harmonic in the customer's current.

Application of the load modeling tool shows that the 9^{th} harmonic current is caused by both the customer and the utility and not just by the customer alone.

V. CONCLUSIONS

If individual harmonic current injections were known, then a utility could penalize the offending customer in some appropriate way, including say a special tariff or insist on corrective action by the customer. Simply measuring the harmonic currents for each individual customer is not sufficiently accurate since these harmonic currents may be caused by not only the nonlinear load, but also by a nonsinusoidal PCC voltage.

This paper demonstrated the ability of MLPNs to learn the admittance of the customer load using actual field data and utilize a trained neural network for estimating the true harmonic distortion caused by that customer. The advantages of this method are that it can be implemented online without disrupting the operation of any load, since only voltages and

currents need to be measured; it does not require any special instruments, and it does not need to make any assumptions about any quantities, e.g. the impedance of the source, or a sine-wave PCC voltage. Every customer has individual power meters which are already receiving the waveforms of voltage and currents and hence it is a feasible option to implement the scheme for each customer individually.

Standards like IEEE 519 provide guidelines for regulating harmonic distortion levels that divide the responsibility between the utility and the customer. The utility has to maintain voltage distortion at the PCC below the specified limits and the customer has to limit the amount of harmonic current injection onto the utility system. However, when certain unusual events like resonance occur in a power system, for instance, the load modeling tool provides a starting point for the troubleshooting to detect the origin of the problem. The information provided by the new method regarding the true current distortion of a load could be used to persuade an offending customer to take steps to mitigate an unacceptably high level of distortion.

The load modeling tool is designed in software and hence can be integrated into any existing power quality diagnostic instrument or be fabricated as a standalone instrument that could be installed in substations of large customer loads, or used as a hand-held clip on instrument.

ACKNOWLEDGMENT

The authors wish to thank Georgia Power Company for providing the field data and technical assistance required for this paper. Financial support by the National Electric Energy Testing Research and Applications Center (NEETRAC), USA for this research work is greatly acknowledged.

REFERENCES

[1] G.T. Heydt, S.P. Hoffman, A. Rishal, R.I. Sasaki, and M.J. Kemper, "The impact of energy saving technologies on electric distibution system power quality," in *Proceedings of the IEEE International Sysmposium of Industrial Electronics (ISIE 1994)*, Santiago, Chile, pp. 176-181, May 25-27, 1994.

[2] W.M. Grady, A. Mansoor, E.F. Fuchs, P. Verde, and M. Doyle, "Estimating the net harmonic currents produced by selected distributed single-phase loads: computers, televisions, and incandescent light dimmers," *IEEE Power Engineering Society Winter Meeting, 2002*, Vol. 2 , 27-31 Jan. 2002, pp. 1090 – 1094.

[3] IEEE Power System Harmonic Working Group, "Bibliography of Power System Harmonics, Part I and II," in *Proceedings of the IEEE PES Winter Power Meeting 1984*, pp. 2460 – 2479, Jan/Feb 1984.

[4] IEEE Standard 519-1992, IEEE Recommended Practices and Requirements for Harmonic Control in Electric Power Systems.

[5] T. Hoevenaars, K. LeDoux and M. Colosino, "Interpreting IEEE STD 519 and meeting its harmonic limits in VFD applications," in *Proceedings of the IEEE Industry Applications Society 50th Annual Petroleum and Chemical Industry Conference,* Houston,Texas, pp. 145 – 150, Sep 15-17, 2003.

[6] W. Xu, and Y. Liu, "A Method for Determining Customer and Utility Harmonic Contributions at the PCC," *IEEE Transactions on Power Delivery*, Vol. 15, Issue 2, pp.804-811, April 2000.

[7] K. Srinivasan, "On Separating Customer and Supply Side Harmonics," *IEEE Transactions on Power Delivery*, Vol. 11, Issue 2, pp. 1003 - 1012, April 1996.

[8] F.Z.Peng, H. Akagi, and A. Nabae, "A novel harmonic power filter," in *Proceedings of the IEEE Power Electronics Specialist Conference (PESC 1988)*, Kyoto, Japan, vol. 2, pp. 1151- 1159, April 11-14, 1988.

[9] F.Z.Peng, H. Akagi, and A. Nabae, "Compensation characteristics of the combined system of shunt passive and series active filters," in *Proceedings of the IEEE Industry Applications Society Annual Meeting (IAS 1989),* San Diego, California, vol. 1, pp. 959 - 966, Oct 1 – 5, 1989.

[10] S. Bhattacharya, D. Divan and B. Banerjee, "Synchronous frame harmonic isolator using series active filters," in *Proceedings of the European Power Electronics Conference*, pp. 30 – 35, 1991.

[11] R.C. Dugan, D.T. Rizy, "Harmonic Considerations for Electrical Distribution Feeders," National Technical Information Service, Report No. ORNL/Sub/81-95011/4 (Cooper Power Systems as Bulletin 87011, "Electrical Power System Harmonics, Design Guide")

[12] Z. Huang, W. Xu and V.R. Dinavahi, "A practical harmonic resonance guideline for shunt capacitor applications," *IEEE Transactions on Power Delivery*, Vol. 18, Issue 4, pp.1382-1387, Oct 2003.

[13] H. Fujita and H. Akagi, "A practical approach to harmonic compensation in power systems—Series connection of passive and active filters," *IEEE Transactions on Industry Applications*, vol. 27, pp. 1020-1025, Nov./Dec. 1991.

[14] Po-Tai Cheng, S. Bhattacharya, and D. Divan, "Operations of the dominant harmonic active filter (DHAF) under realistic utility conditions," *IEEE Transactions on Industry Applications*, Vol. 37, Issue 4, pp.1037-1044, July/Aug. 2001.

[15] B. Burton and R.G. Harley, "Reducing the computational demands of continually online-trained artificial neural networks for system identification and control of fast processes," *IEEE Transactions on Industry Applications*, Vol. 34, Issue 3, pp. 589 – 596, May-June 1998.

[16] J. Mazumdar, R. Harley and F. Lambert, "System and method for determining harmonic contributions from non-linear loads," in *Proceedings of the IEEE Industry Applications Society Annual Meeting (IAS 2005),* Hongkong, vol. 4, pp. 2456-2463, Oct 2 – 6, 2005.

[17] Simon Haykin, "Neural Networks – A comprehensive foundation," Prentice Hall, 2nd edition, 1998, ISBN 0-1327-3350-1.

[18] E.B. Baum and D. Haussler, "What size net gives valid generalization?," in *Proceedings of Neural Computation*, Vol. 1, No. 1, pp. 151-160, Spring 1989.